J Mater Sci (2008) 43:1234–1240
DOI 10.1007/s10853-007-2260-z

Ultraporous monoliths of alumina prepared at room temperature by aluminium oxidation

Jean-Louis Vignes · Claude Frappart · Thomas Di Costanzo · Jean-Claude Rouchaud · Leo Mazerolles · Daniel Michel

Received: 8 February 2007 / Accepted: 26 October 2007 / Published online: 3 December 2007

Abstract The oxidation of aluminium through a mercury film usually leads to unorganized filaments or fibrous powders of hydrated alumina. Here, we show that the addition of a small amount of silver in the mercury considerably modifies the growth process, and that large sized monoliths can be obtained through a new process. Regular growth can be maintained at a typical rate of 2.1 μm s^{-1} (∼0.75 cm/h) for several hours. The samples consist of tangled nanometric fibres and have an open porosity of 99%. The influence of various parameters has been studied and optimal conditions for regular growth have been determined. Anhydrous alumina monoliths with a nanometric microstructure and a high-specific area are obtained after thermal treatments that remove water.

Introduction

The oxidation of aluminium upon exposure to air through a mercury film has been well known for nearly a century [1]. The insuing corrosion could cause the full and fast destruction of aluminium pieces [2, 3]. The as-obtained products, usually called "fibrous aluminas", are amorphous and their microscopic observation reveals that they consist of an array of fibres with a nanometric diametre. Their water content is close to 40% and their bulk density is about 13 kg m^{-3} [4]. The growth of "fibrous aluminas" is highly exothermic and only occurs in the presence of moisture [4–6]. Pinnel and Bennet reported that mercury plays several roles in the corrosion process of aluminium. First, liquid mercury prevents intimate contact of the aluminium with oxygen and consequently inhibits the growth of a passivating oxide layer. In addition, mercury dissolves aluminium without formation of an intermetallic compound and provides a liquid medium allowing the rapid diffusion of Al atoms towards the surface [4]. A thin continuous layer of hydrated alumina is formed in a first step [7], but the organization between fibres rapidly disappears as growth proceeds. As a result, the final corrosion product consists of more or less separated filaments or in a hydrated alumina powder.

During a tutorial experiment on Al oxidation, we observed that the presence of silver in mercury significantly modified the growth rate and the microstructure of the final product. By studying this effect, we determined the conditions required for the preparation of monolithic pieces of porous hydrated alumina [8, 9]. With the controlled conditions reported in experimental section, it is thus possible to produce monoliths continuously at a regular growth rate over several hours.

Successful experiments have been performed on aluminium pieces of various shapes (plain or annular disks, rectangular plates and grids). The resulting monolith has a prismatic shape with its section which is the template of the metallic precursor. Figure 1 shows for instance various images obtained during the growth on a rectangular aluminium plate with an array of holes (Fig. 1a). After treatment of this grid, growth starts perpendicular to the surface and continues during several hours (Fig. 1b–h).

J.-L. Vignes (✉)
Laboratoire d'Ingénierie des Matériaux et des Hautes Pressions, UPR 1311 du CNRS et Université Paris 13, 99 Av J-B Clément, Villetaneuse 93430, France
e-mail: vignes@limhp.univ-paris13.fr

C. Frappart · T. Di Costanzo · J.-C. Rouchaud · L. Mazerolles · D. Michel
Centre d'Etudes de Chimie Métallurgique, UPR 2801 du CNRS, 15 rue G. Urbain, Vitry-sur-Seine Cedex 94407, France

A regular growth rate is observed during about 10 h and then increases slightly (Fig. 2). The resulting monolith presents a regular array of parallel channels as shown on Fig. 3b. In order to obtain a constant diameter for these channels, it is needed to fill the holes of the aluminium plate with a polymer resin.

Experimental

Synthesis of monoliths

Most of the experiments were carried out using rolled aluminium with a very high purity (Goodfellow, >99.999%) or samples cut from cast ingots without post-rolling supplied by Alcan (Mercus, France) or prepared in the CECM. The starting precursor is an aluminium plate, which can have any shape, but needs to be flat. The maximal size used was a 100 × 100 mm plate of high purity aluminium. In a first step, the alumina passivation layer on the side of the plate that will be exposed to humid air is removed by dissolution in a sodium hydroxide solution (2 mol L^{-1}) for 2 min. After rinsing, the Al surface is treated with a solution containing silver and mercury ions. A typical treatment is to dip it for a minute into an aqueous solution containing nitric acid (2 mol L^{-1}), mercury (0.05 mol L^{-1}) and silver (0.01 mol L^{-1}) nitrates. In this way, a liquid mercury–silver film coating the Al surface is produced. After rinsing and drying, the aluminium plate is introduced into a climatic cabinet (Weiss Technik T 130), in order to control temperature and hygrometry during the

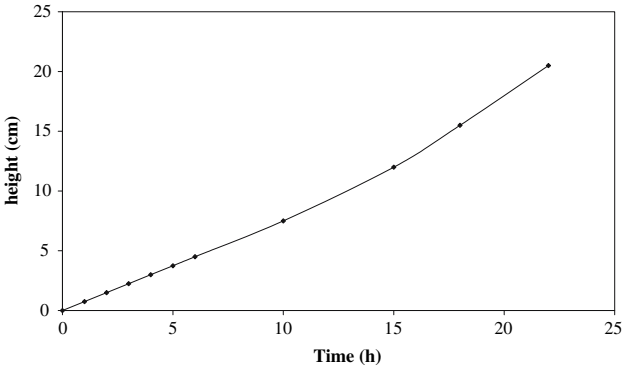

Fig. 2 Monolith growth versus time with the conditions given in the caption of Fig. 1

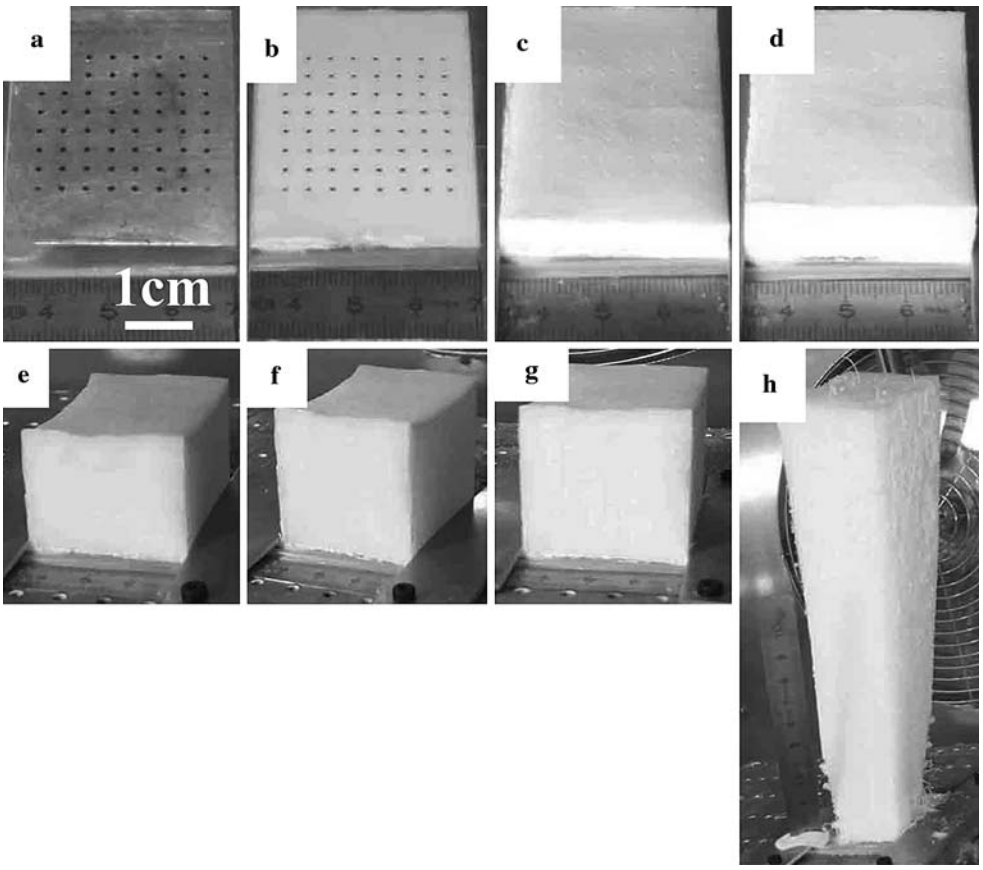

Fig. 1 (**a**) Aluminium grid before alumina growth, (**b**) alumina monolith after a 10 min. growth (20 °C, relative humidity 70%, treatment during 1 min. in a 0.05 mol L^{-1} mercury and 0.01 mol L^{-1} silver nitrate solution), (**c**–**g**) after respectively 1, 2, 4, 5 and 6 h growth, (**h**) alumina monolith after having continued growth for 16 h

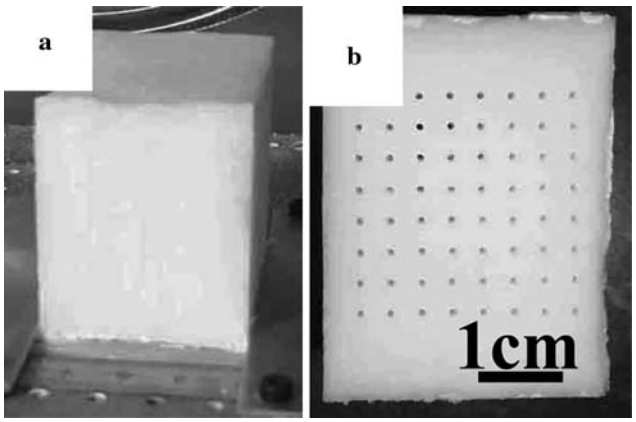

Fig. 3 Alumina monolith after a 6 h growth, (**a**) front view, (**b**) top view

process. The untreated side of the Al plate is fixed on a water-cooled duralumin holder. Stable growth requires the temperature of the aluminium sample not to increase and this cooling device evacuates heat coming from the exothermic oxidation process. The growth rate depends on the Ag/Hg ratio, the temperature, the humidity and the crystal orientation of the aluminium substrate. A typical value obtained at 20 °C with 70% humidity is 2.1 μm s^{-1}. A sample with a given length can be removed during the process using a razor blade-type tool at the level of the amalgam liquid surface. After removing the sample, a new monolith immediately restarts without another amalgamation treatment. The process stops when the whole Al precursor with 1 mm of thickness has been consumed. For instance, a 1-mm thick aluminium plate has produced an accumulated height of about 0.5 m after several days.

Characterization

The crystal structure of alumina samples was studied by X-ray diffraction using a Philips PW 1830 diffractomer (Co-K_α radiation selected by a back monochromator). Chemical analysis were performed by ICP (Inductively Coupled Plasma) using a plasma emission spectrometer (Thermos Can 25, Jarrel-ASH). Transmission electron microscopy studies were conducted on a 200 kV JEOL 2000 FX microscope and scanning electron microscopy studies on a LEO DSM 982 Gemini microscope. Specific areas were measured using a Coulter SA 3100 apparatus.

Results and discussion

Characterization of the monoliths

The product is a hydrated alumina containing 40 to 43 wt.% of water. X-ray diffraction reveals an amorphous structure. The microstructure consists of tangled hydrated alumina fibers with a diameter of about 5 nm (Fig. 4). Inset, the electron diffraction pattern of the observed area is consisting of halos without diffraction spots which confirms the amorphous structure of the material. Samples display a high porosity of about 99% and their bulk density ranges from 15 to 25 kg m^{-3} depending on synthesis conditions. The specific surface area, measured after heating at 350 °C to remove adsorbed humidity, is typically about 300 m^2 g^{-1} with an average size of 10 nm for the mesopores.

Due to their ultralight structure, the monoliths are very brittle. In addition, they are destroyed by the permeation of an aqueous solution. In most of cases, they need to be stabilised by applying a thermal treatment before handling them. This leads to anhydrous alumina, which is amorphous up to 870 °C and to the cubic γ-form above this temperature determined by differential thermal analysis. At higher temperatures, θ and α alumina are successively obtained (Fig. 5). A fine grain microstructure in the range

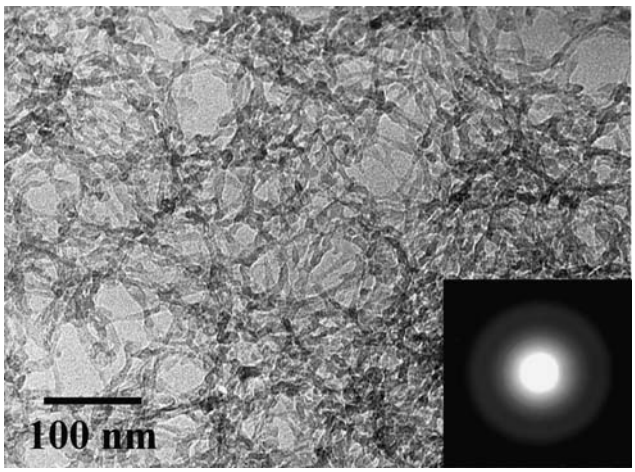

Fig. 4 Transmission electron microscopy image of the fibrous microstructure of a monolith (inset : electron diffraction pattern of the observed area)

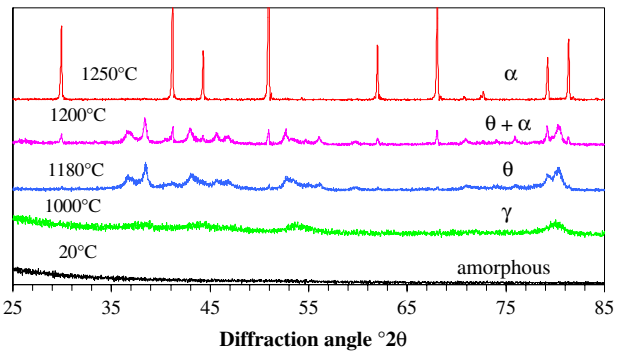

Fig. 5 X-ray analysis on samples treated at different temperatures during 4 h

of 10–20 nm and a high specific area (>50 m^2 g^{-1}) persist up to 1,150 °C (Fig. 6).

The temperatures that we observed for the phase transformations of alumina are higher than that usually reported [10–12]. In our case, the specific fibrous microstructure limits grain growth and therefore can raise the crystallization and the phase transformation temperatures. In particular, the formation of α-alumina is only observed after a sufficient coarsening to a critical size of 20–30 nm [11].

A significant grain coarsening occurs above this temperature after transformation into α-alumina (Fig. 7). Despite shrinkage, the overall shape is kept after the thermal treatments without cracking of the samples (Fig. 8). The linear shrinkage amounts 50% after a 12 h annealing at 1,000 °C, and 85% after a 2 h annealing at 1,600 °C (Fig. 8).

Influence of the aluminium composition

As the process involves the dissolution of aluminium into the silver–mercury film, the impurities, which are soluble in Hg concentrate in this liquid phase. For this reason, the process does not work satisfactorily with commercial aluminium and requires a sufficiently pure Al (>99.99%). The role of the main impurities of aluminium, namely Cu, Si, Mg and Fe, was studied on alloys especially prepared in the CECM by melting under helium atmosphere or supplied by Alcan (Mercus, France). The composition and the origin of the various batches studied are shown in Table 1.

Good quality monoliths, with similar characteristics and the same growth rate were prepared from the two samples which display the highest purities (99.999 and 99.99%). Starting from a 1-mm thick Al sheet, we observed continuous growth up to complete oxidation with the 99.999% sample. In the case of the 99.99% sheet, the oxidation process stopped after about 0.5 mm consumed thickness.

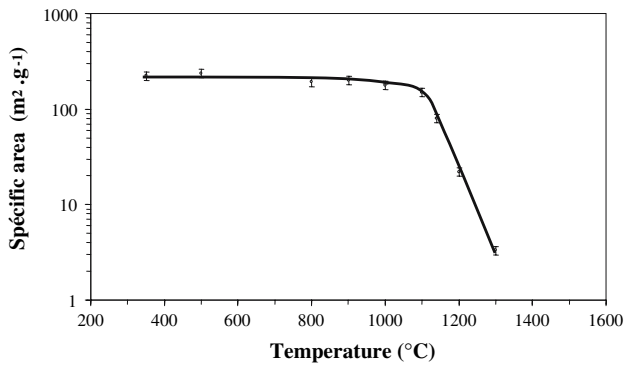

Fig. 6 Variation of the specific area versus temperature. Samples were annealed 4 h at each temperature

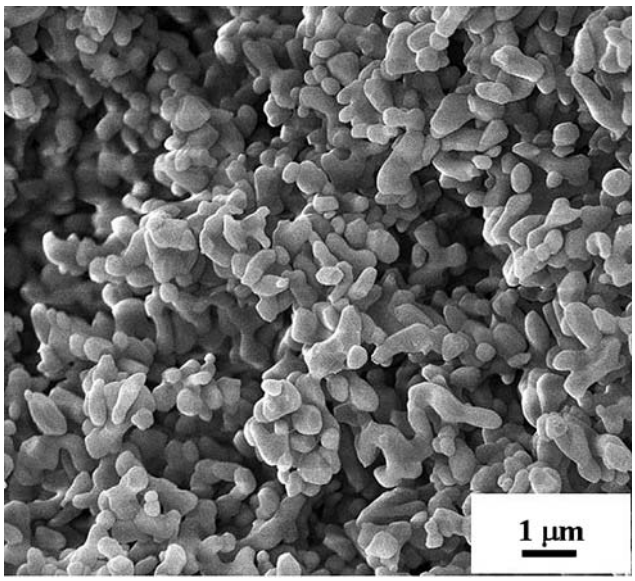

Fig. 7 Scanning electron microscopy image of a monolith after heating 4 h at 1250 °C

For the experiments carried out on CU, SI and FE samples, which were doped with copper, silicon and iron, respectively, a monolith only grew correctly only for few millimeters. Subsequently, isolated fibres are obtained and the process stops. The quantitative analysis of Cu, Si, Fe showed that no trace of these elements was found in the hydrated alumina. As silicon and iron display a very low solubility in mercury, the wetting of the surface by mercury is modified by the gathering of these species at the surface of the Al plate. The solubility of copper in mercury is close to that of aluminium and in this case a solid compound Cu_7Hg_6 is formed when the concentration of copper exceeds the solubility limit. The process stops because liquid mercury is consumed due to the precipitation of Cu_7Hg_6.

A different result was found with the MG1 and MG2 samples doped with magnesium. In these cases, monoliths grew much longer than in experiments with the previously reported impurities. Oxidation of a 1 mm thick Al plate stopped after consuming respectively about 0.5 mm and 0.2 mm. The ICP analysis of the oxidation product gives respectively 0.69% and 1.50% Mg/Al contents. This indicates that magnesium is oxidized simultaneously with Al, but that its oxidation reaction is not complete and is limited to about 78%. Even though the Mg solubility in mercury is much higher than that of the other elements, saturation can be reached, at which point liquid mercury is eliminated by precipitation of the Hg_2Mg compound in agreement with the phase diagram [13]. The presence of magnesium leads to the formation of α-alumina and $MgAl_2O_4$ spinel after heating at 1,300 °C as observed by X-ray diffraction.

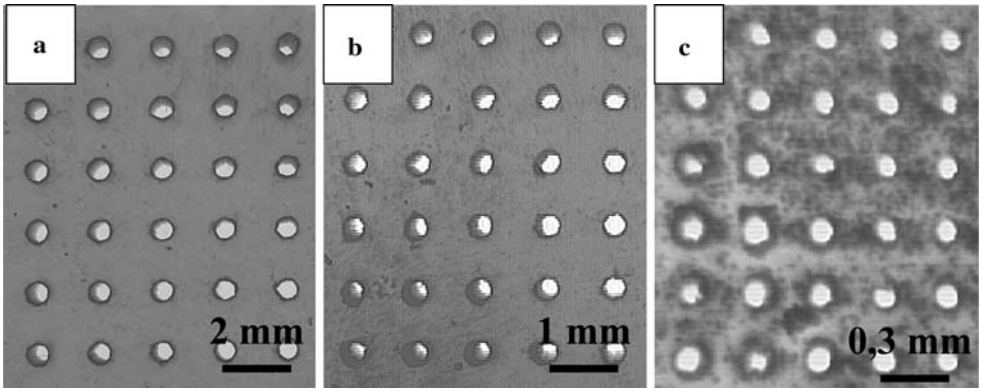

Fig. 8 Evolution of alumina monoliths after heating (**a**) as prepared material, (**b**) after a 12 h heating at 1,000 °C, (**c**) after a 2 h heating 1,600 °C

Table 1 Labelling, origin and composition of the Al precursors

Samples	Cu (ppm in weight)	Si (ppm in weight)	Fe (ppm in weight)	Mg (ppm in weight)
99.999% (Goodfellow)	<2	<1.8	<0.7	<1.5
99.99% (Alcan)	31	26	18	3
CU (Alcan)	4,900	0.3	0.4	0.6
SI (Alcan)	0.3	8,500	0.5	0.2
FE (Alcan)	<1	<1	1,000	<1
MG1 (CECM)	0.3	0.7	0.8	8,800
MG2 (CECM)	<1	<1	<1	19,000

Influence of the crystallographic orientation of the aluminium surface

Several growth experiments were performed on aluminium plates cut from aluminium ingots prepared by casting without rolling. Examination of the Al surfaces with X-ray diffraction using the Laue method has shown that they consisted of grains with random crystallographic orientations. The typical grain size was a few millimeters. We observed that the growth rate of porous alumina depended on the crystalline orientation of Al grains. The most slowly oxidized Al grains correspond to the (111) orientation of surfaces whereas grains with (100) surfaces are the most quickly corroded. As a result, the hydrated alumina samples consist of columnar blocks with various heights. The effect of crystallographic orientation of the aluminium surface was studied on monocrystalline oriented plates coming from an aluminium single crystal (30 cm × 4 cm × 2.5 cm) grown by zone melting at the CECM. The orientation of the specimens was controlled using the Laue method. After cutting, samples were polished and chemically cleaned in order to eliminate surface damage.

With the same experimental conditions, the growth rates of hydrated alumina monoliths were 1.4, 2.2 and 3.3 μm s^{-1} corresponding to the orientations (111), (100) and (110), respectively. The higher the density of aluminium atoms at the surface, the lower the growth rate, but the resulting monoliths displayed nearly the same bulk density 26, 25 and 32 kg m^{-3}, respectively.

Good quality monoliths require a unique orientation of the Al grains. This is the case of monocrystalline or heavily textured polycrystalline surfaces. This condition is satisfied for rolled aluminium plates which display a very strong {100} texture.

Influence of the aluminium surface treatment

When the oxidization of aluminium is performed through a film of pure mercury, the growth rate of hydrated alumina is very high (about 10.6 μm s^{-1}) and it is very difficult to maintain a monolithic growth process during more than a few minutes. Adding silver to liquid mercury slows down the dissolution of aluminium and allows better control of the oxidation reaction.

For instance when the Ag^{+} content of the treatment solution increases from 1.10^{-4} to 1.10^{-2} mol L^{-1}, the growth rate decreases from 3.3 to 2.1 μm s^{-1} and the density of monoliths increases from 15 to 25 kg m^{-3}. As the product of the density and the growth rate remains constant, the corrosion rate of aluminium does not vary with amalgam composition.

The redox potential values of Hg^{2+}/Hg and Ag^{+}/Ag couples are very close and consequently, Hg and Ag metals are simultaneously deposited when their ions are reduced by Al. The thickness of amalgam deposit, after 1 min of treatment, is about 1 μm. Chemical analyses of the Al surface after treatments with a low Ag^{+} concentration solution (between 1.10^{-4} and 1.10^{-3} mol L^{-1}) indicate that the Ag/Hg atomic ratio is lower than 1%. At this composition, the amalgam is mainly formed by a liquid phase according to the Ag-Hg phase diagram [13].

However, after treatment using solutions with a higher Ag content, the amalgam consists of Hg_3Ag_2 crystallites and of liquid mercury saturated in Ag. For instance, treating Al with a 8.10^{-3} mol L^{-1} Ag^{+} solution leads to 25 atom% Ag in the amalgam. The occurrence of the Hg_3Ag_2 phase has been checked by X ray diffraction. The presence of precipitates emerging from the liquid leads the creation of micrometric size channels parallel to the growth direction inside the monolith (Fig. 9).

For silver solutions with higher concentrations (>1.10^{-2} mol L^{-1}), the Ag/Hg deposited composition reaches or exceeds that of the Hg_3Ag_2 alloy. As only solid phases are formed on the Al surface, the oxidation process involving liquid mercury is therefore no longer possible.

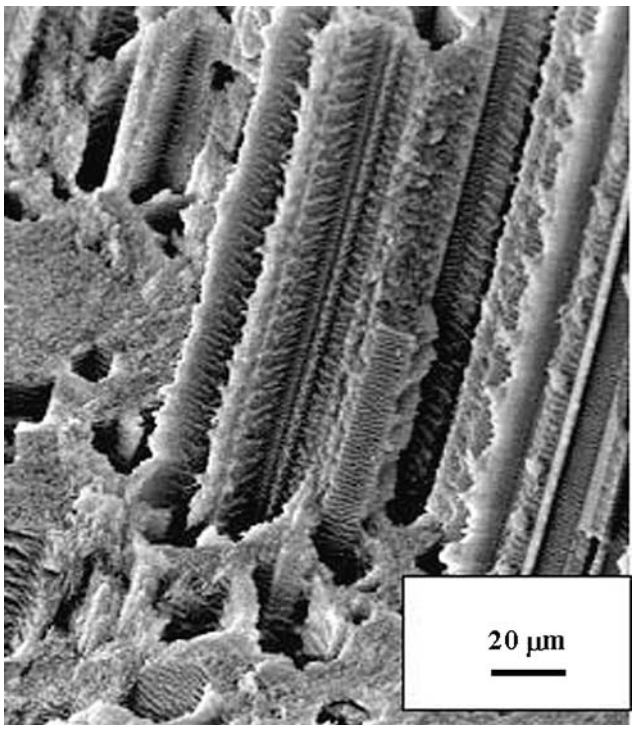

Fig. 9 Scanning electron microscopy of the alumina monolith, view of the channels

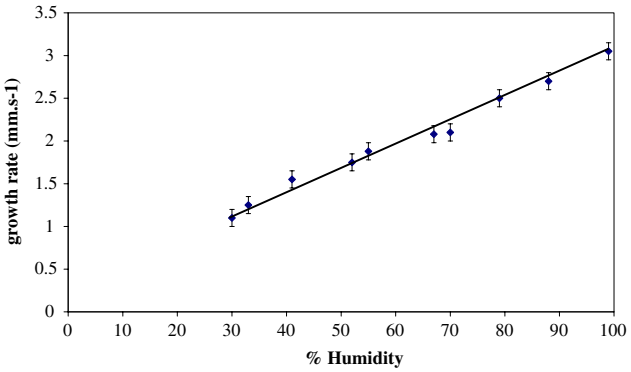

Fig. 10 Curve of the growth rate of hydrated alumina versus humidity at 20 °C

Influence of the humidity of atmosphere

The presence of water is necessary for the growth of monoliths. A humidity level higher than 25%, at 20 °C, is required and the growth rate increases linearly with humidity (Fig. 10). However, the characteristics of final monoliths are similar, irrespective of the humidity during their preparation.

Conclusions

The materials obtained are characterized by a high open porosity resulting mainly from a network of tangled alumina fibers forming pores with an average size of 10 nm. In addition, channels with a micrometric size are formed parallel to the growth direction. This porosity allows an easy access for liquid solution or gaseous phases. Various species can thus be incorporated into the monoliths in a controlled and homogeneous way. Introducing metallic oxide or metal nanoparticles after hydrogen reduction [14–16] has led to prepare efficient catalysts for skeletal isomerization of hexanes and hexenes [17, 18] and for the preparation of carbon nanotubes by chemical vapour deposition [19]. Similar catalysts can be also used for reforming of methane [20], for the hydrodesulfurization of fuels [21] or for the epoxidation of alkenes using hydrogen peroxide [22]. We have also prepared various nanometric porous oxide compounds like spinels or mullite. They are obtained after impregnation of porous alumina by silica, nickel or magnesia salts and subsequent reaction [15, 16].

Other fields for applications of such highly porous aluminas can be foreseen. For instance, it is known that the dispersion of magnetic nanoparticles in the dielectric material induces interesting properties for high-frequency magnetic recording [23, 24]. The high porosity allows also the chemical modification of the surface of the alumina fibers, similarly as it is made in devices used in gas sensors,

particularly for toxic gas detection and pollution monitoring [25]. The special microstructure of highly porous alumina monolith which greatly facilitates exchanges with surrounding media can be beneficial in the field of biosensors or biocatalysts as in the case of mesoporous silicas. For instance, many works were achieved, for instance to trap enzymes [26–29].

Acknowledgements The authors are grateful to Mr. Dubos and Mr. Leroy from the Centre de Recherche Pechiney-Alcan (Voreppe, France) and Mr. Fernandez (Alcan, Mercus, France) for supplying us with high-purity and doped aluminium samples.

References

1. Wislicenus H (1908) Kolloid-Z 2:11
2. Brown MH, Binger WW, Brown RH (1952) Corrosion 8:155
3. Bodle WW, Attari A, Serauskaus R (1986) In: Proceedings of sixth international conference on liquified natural gas, Kyoto, Japan, p 1
4. Pinnel MR, Bennet JE (1972) J Mater Sci 7:1016, doi: 10.1007/BF00550065 10.1007/BF00550065
5. Watson JHL, Vallejo-Freire A, De Souza Santos P, Parsons J (1957) Kolloid-Z 154:4
6. Bruce LA, West GW (1974) J Mater Sci Lett 9:335
7. Markel EJ, Reddick E, Napper LA, Van Zee JW (1994) J Non-Cryst Solids 180:32
8. Beauvy M, Vignes J-L, Michel M, Mazerolles L, Frappart C, Di Costanzo T, patent (CNRS-CEA) n°FR2847569, 28-05-2004
9. Vignes J-L, Mazerolles L, Michel D (1997) Key Eng Mater 132–136:432
10. Iler RK (1961) J Am Ceram Soc 44:618
11. Badkar PA, Bailley JE (1976) J Mater Sci 11:1794, doi: 10.1007/BF00708257 10.1007/BF00708257
12. Levin I, Brandon D (1998) J Am Ceram Soc 81:1995
13. Massalski TB (1990) Binary alloy phase diagrams, 2nd edn. A.S.M. Int. Materials Park, Ohio, vol 3, p 2138, vol 1, p 43
14. Huang Z-R, Jiang D, Michel D, Mazerolles L, Ferrand A, Di Costanzo T, Vignes J-L (2002) J Mater Res 17:3177
15. Mazerolles L, Michel D, Di Costanzo T, Vignes J-L (2002) Ceram Trans 135:227
16. Mazerolles L, Michel D, Vignes J-L, Di Costanzo T, Huang Z, Jiang D (2003) Ceram Eng Sci Proc 24:105
17. Logie V, Maire G, Michel D, Vignes J-L (1999) J Catal 188:90
18. Di Gregorio F, Keller V, Di Costanzo T, Vignes J-L, Michel D, Maire G (2001) Appl Catal A Gen 218:13
19. Bai BJ, Vignes J-L, Fournier T, Michel D (2002) Adv Eng Mat 4:701
20. Raberg LB, Jensen MB, Olsbye U, Daniel C, Haag S, Mirodatos C, Olafsen Sjastad A (2007) J Catal 249:250
21. Dumeignil F, Sato K, Imamura M, Matsubayashi N, Payen E, Shimada H (2005) Appl Catal A Gen 287:135
22. Rinaldi R, Fujiwara FY, Holderich W, Schuchardt U (2006) J Catal 244:92
23. Mazaleyrat F, Varga LK (2000) J Magn Magn Mater 215–216:253
24. Hodama RH (1999) J Magn Magn Mater 200:359
25. Eranna G, Joshi BC, Runthala DP, Gupta RP (2004) Crit Rev Solid State Mater Sci 29:111
26. Cao L, Bornscheuer UT, Schmid RD (1999) J Mol Catal B: Enzym 6:279
27. Tischer W, Kasche V (1999) Trends Biotechnol 17:326
28. Livage J, Coradin T, Roux C (2001) J Phys: Cond Matter 13:R673
29. Nguyen-Ngoc H, Tran-Minh C (2007) Mater Sci Eng C 27:607